Analysis of pulsating electric signals generated in gas-solids pipe flow

S. Matsusaka [a,]*, H. Fukuda [a], Y. Sakura [a], H. Masuda [a], M. Ghadiri [b]

[a] *Department of Chemical Engineering, Kyoto University, Kyoto 615-8510, Japan*

[b] *Institute of Particle Science and Engineering, University of Leeds, Leeds LS2 9JT, UK*

Abstract

In gas-solids pipe flow, particles are electrostatically charged as a result of repeated impacts on the inner walls. When a section of the pipe made of metal is electrically isolated and the charge leakage to the ground is monitored, pulsating electric signals are detected. In the present work, these signals have been studied both experimentally and theoretically. Micrometer-sized alumina particles were dispersed through an ejector and continuously transported in dilute phase. The pipes used were 6 mm in inner diameter, and a pre-charging pipe and detection pipes were installed in the particle transport system. The pulsating electric signals were found to vary in a wide range from positive to negative. The variation of the electric signals was attributed to two electrostatic phenomena (i) the induced current caused by the transport of a cloud of charged particles and (ii) the particle charging caused by repeated impacts on the inner wall. Based on analyses of these phenomena, the total charge, transferred charge, and particle concentration of the cloud can be evaluated. Furthermore, the average velocity of the cloud flowing in the pipe can be obtained from the time interval between peak signals measured with a detection pipe or using a two-detection pipe system based on the correlation method.

Keywords: Electrostatics; Online measurement; Aerosol; Multiphase flow; Particulate processes; Pneumatic conveying

*Corresponding author. Tel.: +81 75 383 2685; fax: +81 75 383 2655

E-mail address: matsu@cheme.kyoto-u.ac.jp (S. Matsusaka).

Introduction

In gas-solids pipe flow, particles are electrostatically charged up to their equilibrium value as a result of repeated impacts on the inner walls (Cole et al., 1969-1970; Masuda et al., 1976). Highly charged particles easily deposit on the inner walls and form a powder layer (Joseph and Klinzing, 1983; Adhiwidjaja et al, 2000, Yao et al., 2004). They also make electrostatic discharges, which can cause fire and explosion hazards particularly for fine powders (Ohsawa, 2003; Nifuku and Katoh, 2003). However, useful information on the state of particles flowing in the transport pipe, such as particle charge, mass flow rate, concentration, and flow velocity, can also be obtained from the electrostatic phenomena caused by charged particles (Yan, 1996; Matsusaka and Masuda 2006; Gajewski, 2006). In general, the electrostatic methods for measurement are classified into two categories, i.e. contact methods based on charge transfer caused by inter-particles and particles-walls collisions (Masuda et al., 1994; Matsusaka and Masuda, 2006) and non-contact methods based on electrostatic induction by means of ring sensors or ring probes (Yan et al., 1995, Gajewski, 2006).

In the present work, we study the electrostatic phenomena caused by impact charging in dilute-phase gas-solids pipe flow, focusing particularly on understanding the origin of pulsating electric signals detected from metal pipes, and discuss the applicability of the electric signals to the analysis of the state of particles flowing in the pipe.

2. Theory of particle charging in gas-solids pipe flow

When a particle impacts on a metal surface, each acquires an equal and opposite charge. The amount of transferred charge by impact decreases with an increase in the charge on the particle; thus, as the number of repeated impacts increases in gas-solids pipe flow, the charge on the particle approaches an equilibrium value (Cole et al., 1969-1970; Masuda et al., 1976). In fully developed gas-solids pipe flows, the number of impacts is proportional to the pipe length and the charge-to-mass ratio, i.e. the specific charge of particles q_{m} can be represented by the following equation (Matsusaka et al., 2007):

$$q_{\mathrm{m}}(L) = q_{\mathrm{m0}} \exp\left(-\frac{L}{L_0}\right) + q_{\mathrm{m}\infty}\left\{1 - \exp\left(-\frac{L}{L_0}\right)\right\} \tag{1}$$

where q_{m0} and $q_{\mathrm{m}\infty}$ are, respectively, the initial and equilibrium charge-to-mass ratios, L is the pipe length, and L_0 is the characteristic length of impact charging. The values of $q_{\mathrm{m}\infty}$ and L_0 depend on the particle properties such as material, size and shape.

When a length of metal pipe is electrically isolated with small dielectric joints and grounded, the charge transferred from the particles to the metal wall flows to the ground. The relationship between the average electric current I and the change in the charge-to-mass ratio of the particles flowing in the pipe is represented by (Masuda et al., 1994; Matsusaka and Masuda, 2006):

$$\frac{I}{W_{\mathrm{p}}} = q_{\mathrm{mi}} - q_{\mathrm{mo}} \tag{2}$$

where W_{p} is the mass flow rate of the particles, q_{mi} and q_{mo} are, respectively, the charge-to-mass ratios of the particles at the inlet and outlet of the metal pipe.

3. Experimental apparatus and procedures

Figure 1 shows a schematic diagram of the experimental apparatus to study the electrostatic phenomena in gas-solids pipe flow. For the experiments, we used spherical alumina particles, 3.1 μm count median diameter, 1.9 in geometric standard deviation, and particle density of 4000 kg m^{-3}. The particles were dried at 110 °C over 12 h and cooled down to room temperature in a desiccator. They were continuously fed with a table feeder (MFOV-1, Sankyo Pio-tech Co., Ltd.) to the test apparatus. To feed the powder at a small flow rate, the particles were directly sucked from the powder layer on the rotating table into a capillary tube less than 1 mm in inner diameter (Matsusaka et al., 2002, 2003). The air was supplied from a compressor and was dried through a condenser, and maintained at a relative humidity of about 10%. The particles were dispersed into the airflow through an ejector (VRL 50-080108, Nihon Pisco Co., Ltd.). The mass flow ratio of the particles to air was less than 1×10^{-3} to ensure that the effect of the particles interactions on the particle charging was negligible. The pipes for pre-charging and detecting electric signals were 6 mm in inner diameter, 0.5, 1, 2, and 3 m long, made of stainless steel (JIS, SUS 304) or copper. The average air velocity in the pipe was 40 m s^{-1}, at which no particle deposit layer was formed and the particles impacted directly on the inner walls. To increase the efficiency of particle charging, the pipes were formed in a spiral shape with a radius of curvature of 80 mm.

The electric current flowing from the metal pipes to the ground was measured with an electrometer. To check the charge balance in this system, the charge-to-mass ratios of particles at the inlet and outlet of the metal pipe were measured by connecting it to a Faraday cage. Also, a digital oscilloscope (NR-350, Keyence Corp.) was used to analyse the high-frequency fluctuations of the electric current. Most experiments were conducted under ambient conditions of 20–25 $^{\circ}$C and 15–30% RH. Some experiments were carried out at higher relative humidity (60–70% RH).

4. Results and discussion

4.1 Charge transfer in gas-solids pipe flow

Figure 2 shows an example of the electric current measured by the electrometer. The average current flowing from a 0.5 m long detection pipe made of copper was positive (≈ 1 nA). The alumina particles were negatively charged by the impacts on the copper surface; hence positive charges flow to the ground through the pipe wall. However, the value of current fluctuated considerably from positive to negative. The origin of the fluctuations is discussed in detail later. Using a detection pipe made of stainless steel, the alumina particles were positively charged and the average electric current to the ground was negative. These trends on the particle charging agree with those reported by Matsusaka et al. (2007).

To check on the charge balance in this system, we measured the charge-to-mass ratios of the particles at the inlet and outlet of the detection pipe q_{mi} and q_{mo}. Figure 3 shows the relationship between the average electric current per unit mass flow rate I/W_p and the change in the charge-to-mass ratio of the particles q_{mi}–q_{mo}. Since the amount of charge flowing to the ground agrees with the change in the charge on the particles, the charge balance on this system holds; thus, the charge transfer between the particles and the metal wall can be evaluated by the electric current. However, high-frequency fluctuations are detected in the measurements of the electric current (see Fig. 2). To clarify the origin of the fluctuations, we measured the electric signals with the digital oscilloscope. Figure 4 shows the voltage recorded with time, where the same trend as that of Fig. 2 is observed; i.e. many pulsating signals are detected. Figure 4(b) shows the variation of the voltage with a magnified time scale. Each pulsating signal in this result consists of negative and positive values.

4.2 Polarity of pulsating electric signals

Figure 5(a) shows a typical pulsating electric signal detected from a 0.5 m long copper pipe, where the alumina particles were pre-charged by another 0.5 m long copper pipe. It is found that the first peak of the voltage is negative and the second one is positive. The variation can be explained as follows (Masuda et al., 1977; Yan et al., 1995 Matsusaka et al., 2000); alumina particles are continuously fed with the table feeder; however, the feed rate fluctuates somewhat on a time scale of milliseconds. As a result, the particle concentration in gas-solids pipe flow also fluctuates, and a number of clouds of particles flow in the pipe. When a cloud of negatively pre-charged particles approaches the detection pipe, positive charges are induced on the inner surface of the pipe. The electrons on the inner surface flow to the ground, i.e. induced current is negative. Since the voltage measured with the digital oscilloscope is equal to the product of the induced current and the electric resistance in this system, the voltage is negative (Fig. 5(b), (1) → (2)). If the electric field caused by the charged cloud is formed only in the detection pipe, the amount of the induced charge will be constant and no induced current flows. Here, it is worth noting that the particles can still obtain negative charges by impacting on the inner surface of the detection pipe, and the wall surface obtains positive charges. Even though the charge transfer occurs between the particles and the wall, the charge balance holds, and no charges flow to the ground. After the particles pass through the detection pipe, the whole positive charges held on the wall surface flow to the ground, and positive voltage is detected (Fig. 5(b), (3) → (4)). Since the positive charges that were transferred from the particles are added to the pre-induced charge, the second peak of the voltage is larger than the first one.

Figure 6(a) shows a different pulsating electric signal, i.e. both peaks of the voltage are positive. Since there is no negative peak, the range of fluctuations of the electric signals will be smaller. When particles that were positively pre-charged by stainless steel pipe approach the detection pipe, negative charges are induced on the inner wall surface of the pipe. Therefore, positive charges on the wall surface flow to the ground, and positive voltage is detected (Fig. 6(b), (1) → (2)). The particles obtain negative charges by impacting on the inner wall of the detection pipe made of copper, and the polarity of the particle charge changes into negative. The electrons are transferred from the wall surface to the particles: consequently, the polarity of the charge on the inner wall surface of the pipe changes into positive. After the particles pass through the detection pipe, the whole positive charges held on the wall surface flow to the ground and positive voltage is detected (Fig. 6(b), (3) → (4)).

The shape of the electric signals depends on the polarity and amount of the charges of the cloud at the inlet and outlet of the detection pipe. All the patterns of particle charging in gas-solids pipe flow and the shapes of the electric signals are illustrated in Fig. 7. Here, it is supposed that the particle charging is represented by an exponential equation (Cole et al., 1969-1970; Masuda et al., 1976, Matsusaka and Masuda 2003, Matsusaka et al., 2007) and that the detection pipe length is larger than the size of the cloud, i.e. the tails of the two peaks do not overlap. Figure 7(a) shows the case that the particles obtain negative charges, and the equilibrium charge is also negative; while Fig. 7(b) shows the case that the particles obtain positive charges, and the equilibrium charge is also positive. The experimental results in Figs. 5 and 6 correspond to the cases of (3) and (2) in Fig. 7, respectively.

4.3 Calculation of the electrostatic charge of a cloud

If the detection pipe is sufficiently long, the total charge of a cloud q at the inlet or the outlet can be calculated using the following equation (Matsusaka et al., 2000):

$$q = \frac{S}{R} = \frac{1}{R}\int_{t_0}^{t_1} V dt \qquad (3)$$

where S is the integration value, R is the electric resistance, V is the voltage, and t is the elapsed time (see Fig. 8). The change in the charge on particles passing through the detection pipe, i.e. the transferred charge, Δq is given by:

$$\Delta q = -\frac{S_\mathrm{i} + S_\mathrm{o}}{R} \tag{4}$$

Figure 9 shows the relationship between the transferred charge and the initial charge of a cloud. These values depend on the particle charging conditions such as the wall material and pipe length. Figure 9 (a) shows the results obtained using the copper pipes for pre-charging and detecting. Since the alumina particles are negatively charged by the impacts on the copper surface, the data are negative, while, for the impacts on stainless steel surface, the data are positive as shown in Fig. 9(b). It is found that the amount of the transferred charge increases with the amount of the initial charge irrespective of the polarity of the charge. This is mainly caused by the distribution of the number of particles in a cloud; i.e., when large number of particles pass through the pipe, the initial charge and the charge transfer are large. It is also found that the amount of the transferred charge decreases with increasing pipe length for pre-charging. This is because the particle charge approaches the equilibrium value with the increase in the pipe length for pre-charging.

Experiments were also carried out under high humidity conditions (Fig. 9(b)), showing that the charges obtained under higher humidity conditions were larger than those under lower humidity conditions. For the higher humidity, agglomerated particles were fed and the number of particles in a cloud increased; thus, the detected charges also increased. However, at very high humidities, the values might decrease because of the reduction in the equilibrium charge even though larger agglomerated particles are fed. Although the effect of moisture on the electrostatic phenomena of particles can be explained qualitatively, it is not easy to quantitatively estimate the effect since there are too many factors influencing the process.

4.4 States of clouds of particles and pulsating signals

Figure 10 shows the electric signals obtained using a 0.5 m long copper pipe. In this experiment, different lengths of copper pipes were used for pre-charging. Since the length of the detection pipe and the fluid velocity are not changed, the time interval between the two peaks is constant. However, the intensity of the electric signals decreases as the pipe length for pre-charging is increased. This is because the velocities of the particles flowing through the pipe are not constant and the particles are more widely spaced within the pipe; i.e. the particle concentration in the clouds is lower than that for the shorter pipe. Therefore, the intensity of the electric signals will give information on the state of the clouds.

Figure 11 shows the effect of the length of the detection pipe on the electric signals. The time interval between the two peaks increases proportionally with the pipe length. This is a reasonable result, and applicable to the measurement of the average velocity of particles in dilute-phase gas-solids pipe flows. The height of the second peak decreases with increasing the pipe length. This is mainly caused by the decrease in the particle concentration as mentioned above.

We also performed an experiment using the correlation method (Yan et al., 1995, Gajewski, 1996). Here, we used two 0.5 m long copper pipes for detecting electric signals and a different length of stainless steel pipe for connecting the detection pipes. The intermediate pipe was electrically isolated with small dielectric joints and grounded. Three sets of electric signals are shown in Fig. 12. Particles that were negatively pre-charged obtain negative charge in the first detection pipe, but the polarity of the charge on the particles changes from negative to positive by passing through the intermediate pipe, and again changes to negative by the second detection pipe. These variations in the particle charge can be explained by the polarity of the electric signals. The time interval between the first and second detection pipes increases proportionally with the length of the intermediate pipe. Therefore, the system is applicable to the measurement of particle velocity based on the correlation method. Also, the intensity of the electric signal decreases with the pipe length because of the particle distribution; hence, the intermediate pipe should not be too long. On the material of the intermediate pipe, there is no special limit unless it makes the particle charge zero.

5. Conclusions

We have analyzed the pulsating electric signals detected from the metal pipes in a dilute-phase gas solids flow system. The results obtained are summarized as follows.

(1) The alumina particles were negatively charged by impacting on copper surfaces and positive charges flowed to the ground, whilst the particles were positively charged by impacting on stainless steel surfaces and negative charges flowed to the ground.

(2) The amount of charge flowing to the ground agreed with the change in the charge on particles.

(3) The electric current flowing to the ground fluctuated considerably from positive to negative. It contained sharp pulses corresponding to the induced current caused by the transport of a cloud of charged particles through the detection pipe. The origin of the variations of the electric signals was attributed to the induced current brought about by particle charging due to repeated impacts on the inner walls.

(4) Using the above analysis technique, the total charge, transferred charge, and particle concentration of the cloud can be evaluated.

(5) The average velocity of the particle cloud flowing in the pipe can be obtained from the time interval between the peak signals at the inlet and outlet of the detection pipe.
(6) Using two detection pipes, the method can be applied to the measurement of particle velocity based on the correlation method.

Notation

I	electric current, A
L	pipe length, m
L_0	characteristic length of impact charging, m
m	mass flow ratio of particles to gas, dimensionless
q	charge of a cloud of particles, C
q_{m}, q_{mi}, q_{mo}	charge-to-mass ratio of particles, C kg^{-1}
q_{m0}	initial charge-to-mass ratio of particles, C kg^{-1}
$q_{m\infty}$	equilibrium charge-to-mass ratio of particles at $L = \infty$, C kg^{-1}
R	electric resistance, Ω
S	integration value, V s
t, t_0, t_1	time, s
V	voltage, V
W_p	mass flow rate of particles, kg s^{-1}
ψ	relative humidity, dimensionless
Subscripts	
i	inlet of detection pipe
o	outlet of detection pipe
pre	pre-charge pipe
det	detection pipe
Greek letter	
Ψ	relative humidity, dimensionless

Acknowledgments

The authors acknowledge the support by Core-to-Core Program for Advanced Particle Handling Science, JSPS. This research was also supported by Kyoto Prefecture Collaboration of Regional Entities for the Advancement of Technological Excellence, JST.

References

Adhiwidjaja, I., Matsusaka, S., Yabe, S., Masuda, H., 2000. Simultaneous phenomenon of particle deposition and reentrainment in charged aerosol flow —effects of particle charge and external electric field on the deposition layer. Advanced Powder Technology 11, 221-233.

Cole, B.N., Baum, M.R., Mobbs, F.R., 1969-1970. An investigation of electrostatic charging effects in high-speed gas-solids pipe flows. Proceedings of the Institution of Mechanical Engineers 184, 77-83.

Gajewski, J.B., 1996. Monitoring electrostatic flow noise for mass flow and mean velocity measurement in pneumatic transport. Journal of Electrostatics 37, 261-276.

Gajewski, J.B., 2006. Non-contact electrostatic flow probes for measuring the flow rate and change in the two-phase gas-solids flows. Chemical Engineering Science 61, 2262-2270.

Joseph, S., Klinzing, G.E., 1983. Vertical gas-solid transition flow with electrostatics. Powder Technology 36, 79-87.

Masuda, H., Komatsu, T., Iinoya, K., 1976. The static electrification of particles in gas-solids pipe flow. A.I.Ch.E. Journal 22 558-564.

Masuda, H., Mitsui, N., Iinoya, K., 1977. Experimental study of the electric pulses generated by flowing gas-solid suspension of low concentration, Kagaku Kogaku Ronbunshu 3, 457-461.

Masuda, H., Matsusaka, S., Nagatani, S. 1994. Measurements of powder flow rate in gas-solids pipe flow based on the static electrification of particles. Advanced Powder Technology 5, 241-254.

Matsusaka, S., Masuda, H., 2003. Electrostatics of particles. Advanced Powder Technology 14, 143-166.

Matsusaka, S., Masuda, H. 2006. Simultaneous measurement of mass flow rate and charge-to-mass ratio of particles in gas-solids pipe flow. Chemical Engineering Science 61, 2254-2261.

Matsusaka, S., Ghadiri, M., Masuda, H., 2000. Electrification of an elastic sphere by repeated impacts on a metal plate. Journal of Physics D: Applied Physics 33, 2311–2319.

Matsusaka, S., Umemoto, H., Nishitani, M., Masuda, H., 2002. Electrostatic charge distribution of particles in gas-solids pipe flow, Journal of Electrostatics 55, 81-96.

Matsusaka, S., Oki, M., Masuda, H., 2003. Bipolar charge distribution of a mixture of particles with different electrostatic characteristics in gas-solids pipe flow. Powder Technology 135-136, 150-155.

Matsusaka, S., Oki M., Masuda, H., 2007. Control of electrostatic charge on particles by impact charging. Advanced Powder Technology 18, 229-244.

Nifuku, M., Katoh, H., 2003. A study on the static electrification of powders during pneumatic transportation and the ignition of dust cloud. Powder Technology 135-136, 234-242.

Ohsawa, A., 2003. Computer simulation for assessment of electrostatic hazards in filling operations with powder, Powder Technology 135-136, 216-222.

Yan, Y., 1996. Mass flow measurement of bulk solids in pneumatic pipelines. Measurement Science and Technology 7, 1687-1706.

Yan, Y., Byrne, B., Woodhead, S., Coulthard, J., 1995. Velocity measurement of pneumatically conveyed solids using electrodynamic sensors. Measurement Science and Technology 6, 515-537.

Yao, J., Zhang, Y., Wang, C-H., Matsusaka, S., Masuda, H., 2004. Electrostatics of the granular flow in a pneumatic conveying system. Industrial and Engineering Chemistry Research 43, 7181-7199.

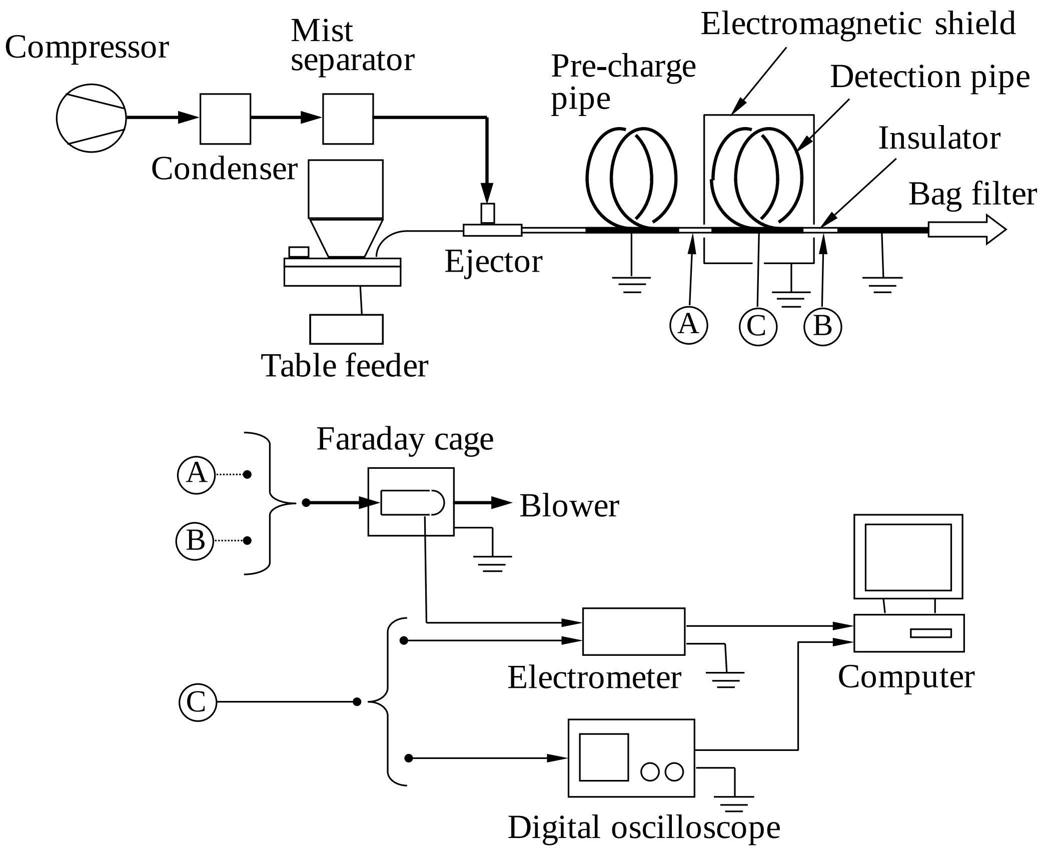

Fig. 1. Experimental apparatus.

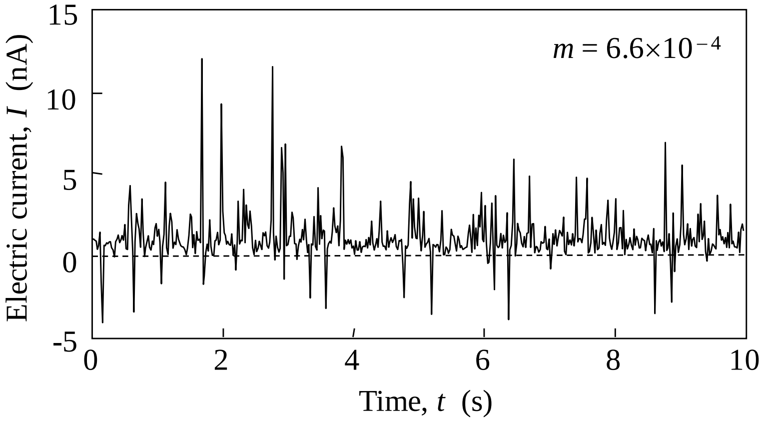

Fig. 2. Electric currents flowing from the detection pipe to the ground, measured with the electrometer (detection pipe: copper, L_{det} = 0.5 m).

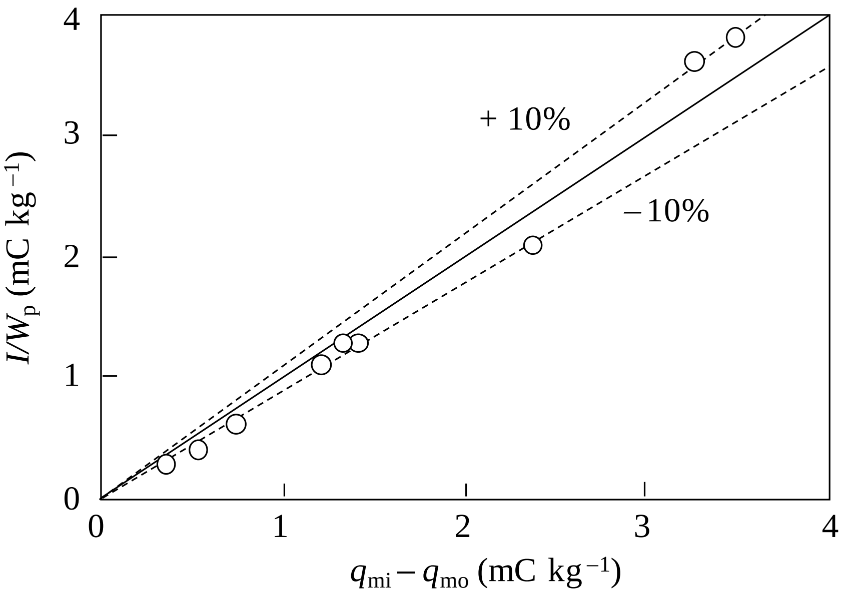

Fig. 3. Electric charge balance (detection pipe: copper, L_{det} = 0.5 m).

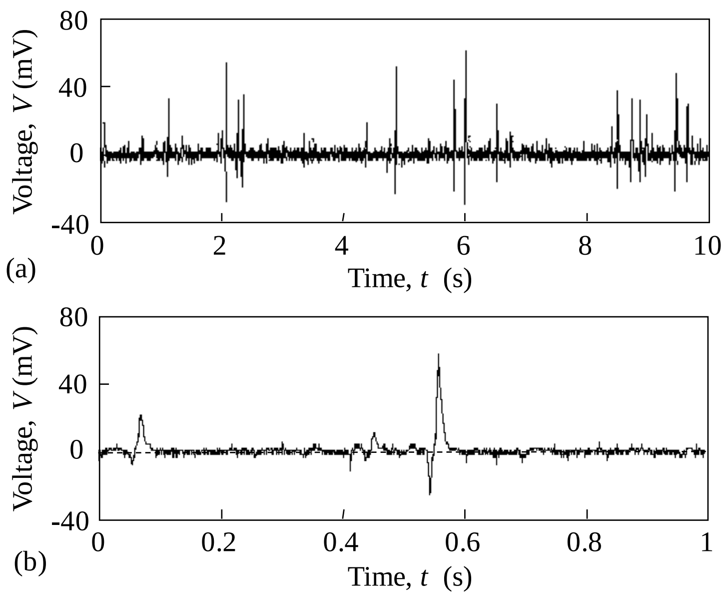

Fig. 4. Voltage of the detection pipe measured with the digital oscilloscope (detection pipe: copper, L_{det} = 0.5m; $m = 4.4\times10^{-4}$).

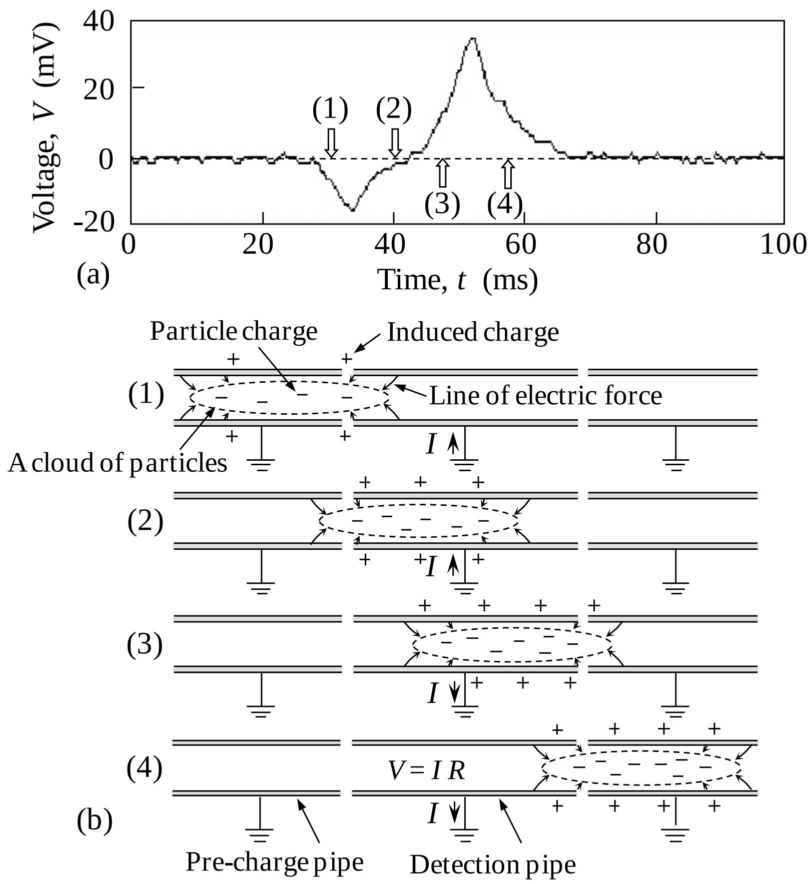

Fig. 5 (a) Shape of an electric signal detected with the digital oscilloscope (Case 1); (b) state of charge transfer (pre-charge pipe: copper, L_{pre} = 0.5 m; detection pipe: copper, L_{det} = 0.5 m).

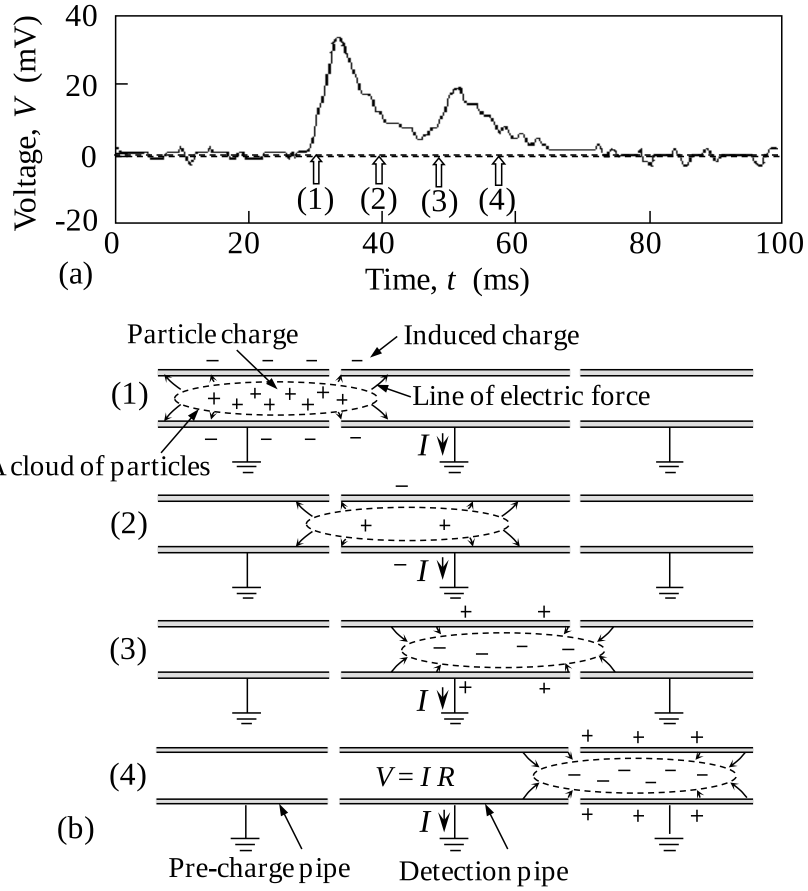

Fig. 6 (a) Shape of an electric signal detected with the digital oscilloscope (Case 2); (b) state of charge transfer (pre-charge pipe: Stainless steel (SUS 304), L_{pre} = 0.5 m; detection pipe: copper, L_{det} = 0.5 m).

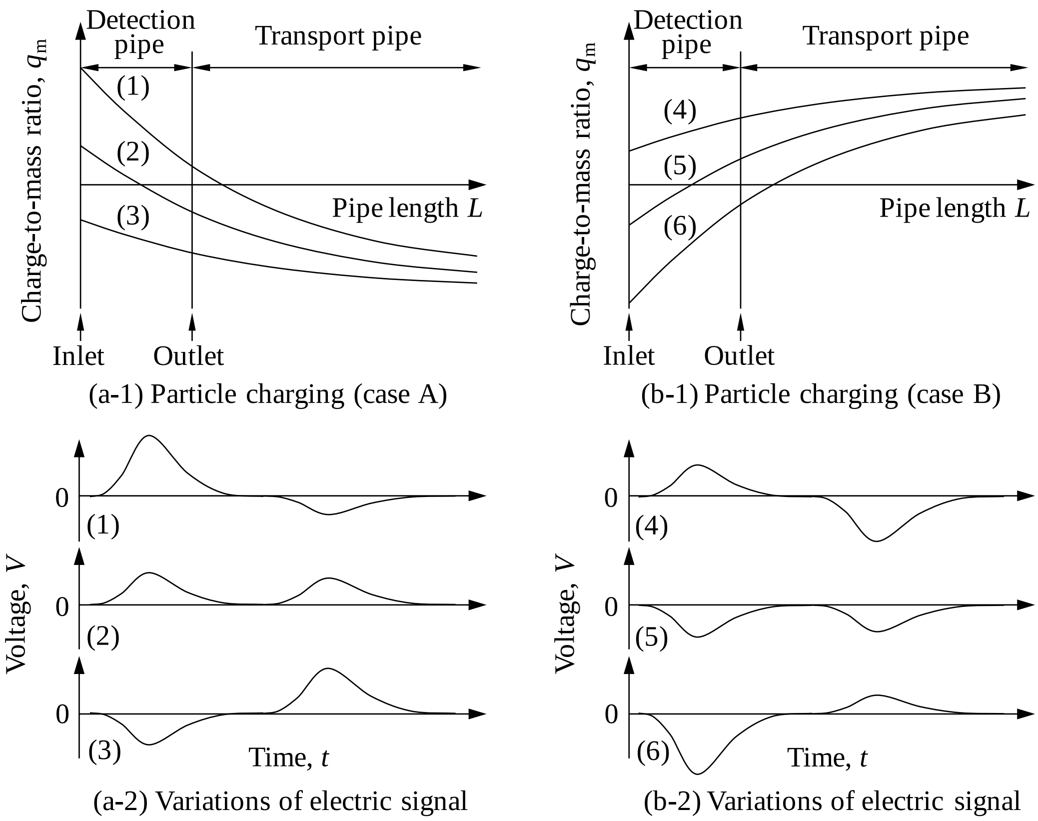

Fig. 7. Effect of particle charging on the shape of electric signal.

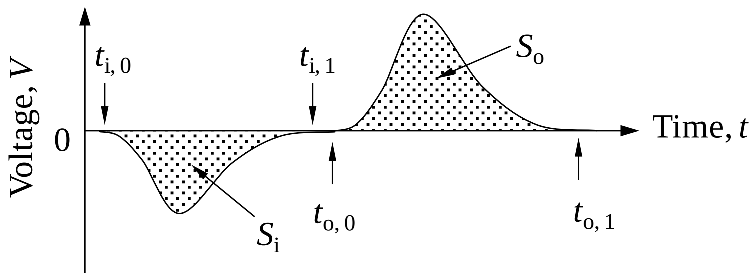

Fig. 8. Calculation of electrostatic charge.

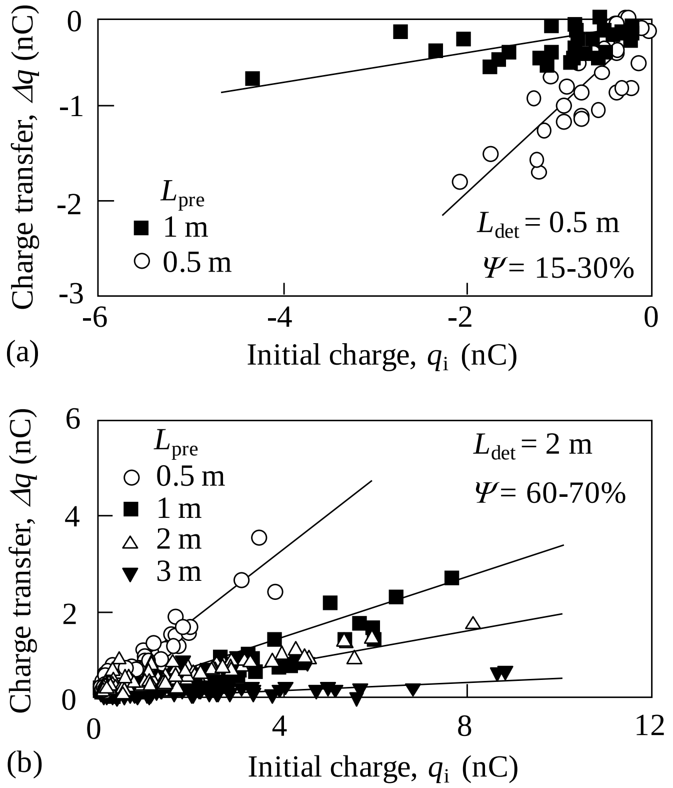

Fig. 9. Effect of the initial charge of a cloud on the charge transfer; (a) pre-charge pipe and detection pipe: copper; (b) pre-charge pipe and detection pipe: stainless steel.

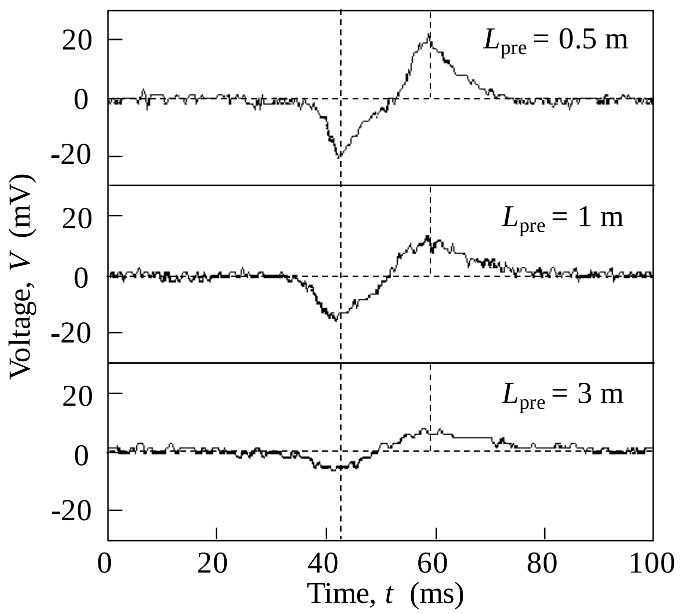

Fig. 10. Effect of the pipe length for pre-charging on the electric signals (pre-charge pipe: copper, detection pipe: copper, L_{det} = 0.5 m).

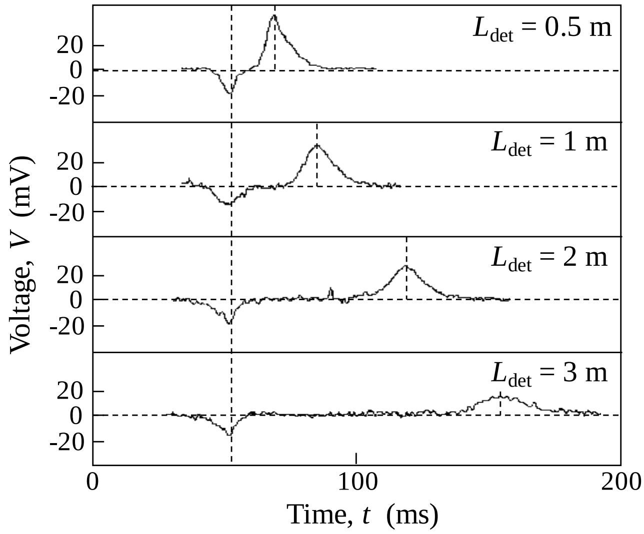

Fig. 11. Effect of the length of detection pipe on the electric signals (detection pipe: copper).

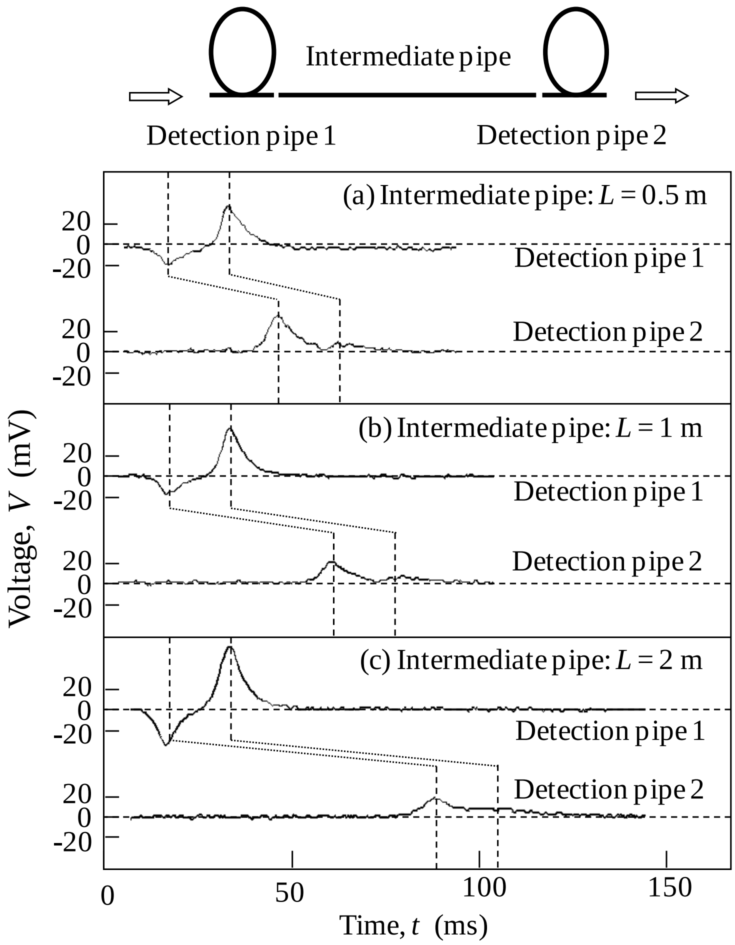

Fig. 12. Electric signals obtained by a two-detection pipe system (detection pipes: copper, L_{det}= 0.5 m; intermediate pipe: stainless steel).